

Evaluation of the effect of the thermomechanical parameters on the chaotic dynamics of shape memory oscillators

Davide Bernardini and Giuseppe Rega

Dipartimento di Ingegneria Strutturale e Geotecnica, Sapienza Università di Roma

E-mail: davide.bernardini@uniroma1.it, giuseppe.rega@uniroma1.it

Keywords: chaos, nonlinear dynamics, thermomechanics, shape memory alloys.

SUMMARY. A systematic study of the effect of various thermomechanical model parameters on the nonlinear dynamical response of Shape Memory Oscillators is carried out in the background of theoretical predictions by the construction of behavior charts. Use is made of the Method of Wandering Trajectories, enhanced by the evaluation, as a quantitative indicator of chaoticity, of the maximum value of the normalized separation in the displacement over a fixed interval of time. It turns out that two main aspects of the model behavior are relevant for the occurrence of chaos: the slope of the pseudoelastic plateaus and the width of the hysteresis loop. It is shown that these two aspects are governed by various combinations of model parameters to be possibly controlled in the design stage in order to avoid undesired dynamic behaviors.

1 INTRODUCTION

A *Shape Memory Oscillator* (SMO) is characterized by a *Shape Memory Device* (SMD) that provides a restoring force against the relative displacements of a pair of points of a main structure [1]. A SMD is composed by an arrangement of *Shape Memory Materials* (SMM) that may be designed to yield various kinds of behavior. In this work the attention is focused on SMDs with pseudoelastic behavior (Fig. 1).

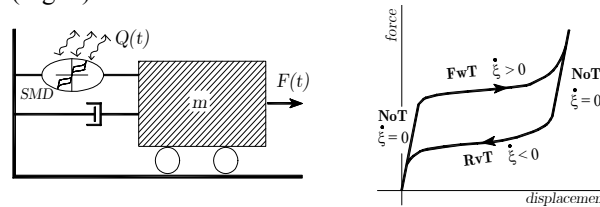


Figure 1: Schematic representation of a SMO (left) and typical pseudoelastic loop of SMD (right)

The pseudoelastic restoring force is modeled by a thermomechanical constitutive law proposed in [2] for the SMM and then adapted in [3] for use in nonlinear dynamics.

The SMOs are considered within a thermomechanical environment characterized by an harmonic forcing excitation $F(t) = \gamma \cos \alpha t$ and a convective heat exchange $Q(\mathcal{G}) = h(\mathcal{G}_e - \mathcal{G})$ where γ and α are the excitation amplitude and frequency, \mathcal{G}_e the environment temperature and h the coefficient of convective heat exchange [3, 6]. At each time t the state of the SMO is described by the vector:

$$\mathbf{u}(t) := [x(t), v(t), \xi(t), \mathcal{G}(t), \xi_0(t)]$$

where $x(t)$, $v(t)$, $\mathcal{G}(t)$ are displacement, velocity and temperature of the device while $\xi(t) \in [0, 1]$ is an internal variable that describes the internal state of the SMM. To model the complex hysteretic

behavior of SMM the state depends not only on the actual value $\xi(t)$ but also on the value $\xi_0(t)$ of ξ at the beginning of the last process of change of ξ occurred before time t . As discussed in [3, 6] the time evolution of the state takes place according to a system of 5 differential equations:

$$\begin{cases} \dot{x} = v \\ \dot{v} = -x + (\text{sgn}(x)\lambda)\xi - \zeta v + F \\ \dot{\xi} = Z[\text{sgn}(x)v - JQ] \\ \dot{g} = ZL\left(\frac{\Lambda}{J\lambda} + \vartheta\right)[\text{sgn}(x)v - JQ] + Q \end{cases}$$

in which Z and Λ are constitutive functions that can take three different expressions depending on suitable state-dependent criteria [1, 3, 6]. The model depends on 7 model parameters $\lambda, J, q_1, q_2, q_3, L, h$ whose physical meaning is discussed later (see also [1]) as well as on the damping coefficient ζ of the viscous damper (Fig. 1).

The nonlinear dynamics of SMOs has been the subject of several studies [3-6] that, among other things, revealed the occurrence of chaotic solutions in various ranges of model parameters. Some preliminary steps towards a systematic investigation of the occurrence of chaos in such systems were carried out by means of bifurcation diagrams in [1] and by the Method of Wandering Trajectories (MWT) in [6].

For a given N -dimensional mechanical system subject to a periodic forcing excitation, the MWT considers a fiduciary trajectory $\mathbf{u}(t)$ starting from the initial condition \mathbf{u}_0 and a perturbed trajectory $\mathbf{u}^*(t)$ starting from an initial condition $\mathbf{u}^* = \mathbf{u}_0 + \varepsilon\mathbf{A}$ where ε is a positive perturbation parameter and \mathbf{A} is the vibration amplitude vector whose i -th component is defined as follows:

$$A_i := \frac{1}{2} |a_i - b_i| \quad \text{where } a_i := \max_{t \in \mathfrak{T}_1} u_i(t) \quad \text{and } b_i := \min_{t \in \mathfrak{T}_1} u_i(t)$$

$\mathfrak{T}_1 := [t_1, T]$ being an observation interval where the transients can be considered to be expired. Once the two trajectories are known over \mathfrak{T}_1 the separation $\mathbf{h}(t) := \mathbf{u}^*(t) - \mathbf{u}(t)$ can be computed and normalized with respect to the vibration amplitude

$$\alpha_i(t) := \frac{|h_i(t)|}{A_i} \quad h_i(t) := u_i^*(t) - u_i(t)$$

At each time, $\alpha_i(t)$ is the i -th component of the *normalized separation vector* $\boldsymbol{\alpha}(t)$ that expresses the divergence between the two trajectories normalized with respect to the vibration amplitude. Since $h_i(0) = \varepsilon A_i$, the initial separations are $\alpha_i(0) = \varepsilon$. If the motion is regular all $\alpha_i(t)$ take values of the order of ε or decay to zero. By contrast, non-regular motions lead to normalized separations much higher than ε that, with the progress of time, level off at the size of the attractor [7].

In [1] a detailed analysis of the model parameters was carried out and some hints about their likely effect on the dynamic response of the SMD were given. In [7] the possibility to enhance the MWT by means of the evaluation of the maximum value α_{\max} of the displacement normalized separation over a fixed observation interval \mathfrak{T}_1 – to be considered as a comparative indicator of chaoticity of non-regular solutions – was suggested.

By plotting α_{\max} as a function of the excitation frequency and/or the excitation amplitude, it is possible to obtain synthetic pictures (behavior charts) – via systematic numerical simulations – that give immediate appreciation not only of the zones in which the chaotic responses occur, but

also of the comparative level of chaoticity of each non-regular solution.

In this paper, after an overview on the physical meaning of the various model parameters, behavior charts for some representative sets of model parameters are obtained numerically in the background of theoretical expectations [1] with the aim to give a systematic description of their effect on the occurrence of chaotic responses in the nonlinear dynamics of SMOs.

2 OVERVIEW OF THE MODEL PARAMETERS

As anticipated in the previous Section, the thermomechanical constitutive model used to describe the restoring force of the SMD depends on the 7 parameters :

$$\lambda, J, q_1, q_2, q_3, L, h$$

that can be grouped as follows:

- **mechanical** parameters (q_1, q_2, q_3, λ), which reflect the basic features of the device (type and arrangement of the material) and determine the basic shape of the pseudoelastic loop as observed in isothermal conditions;
- **thermal** parameters (L, h), which reflect the heat production, absorption and exchange with the environment and therefore determine the temperature variations of the device;
- **thermo-mechanical** parameter J , which determines the influence of the temperature variations on the phase transformation forces.

More details about the physical meaning of such parameters are discussed in [1].

In order to explore the complicated system response, the following set of *Reference Model Parameters* (RMP) is chosen

q_1	q_2	q_3	λ	L	h	J
0.98	1.2	1.0167	8.125	0.12	0.08	3.1742

Table 1: Reference Model Parameters (RMP) considered in the comparative analysis.

The viscous damping as well as the parameter b [1] are set to 0.03 for each analysis. Several variations of the parameters with respect to RMP will be studied later.

Before discussing the various sets of parameters considered in the investigation, a few basic features of the response of the SMD characterized by the RMP is recalled. Since the mechanical response depends on the loading rate, two typical responses of the same SMD under a smaller and a faster loading are shown in Figure 2.

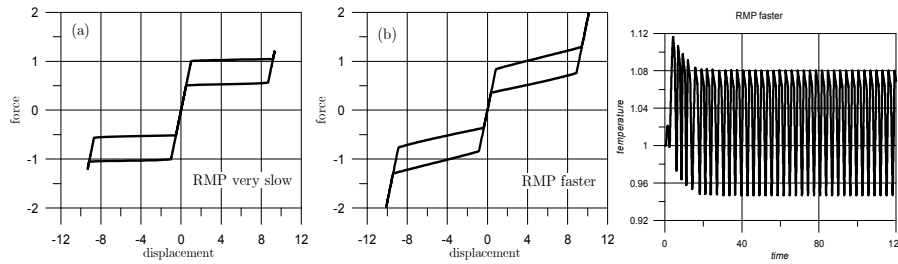


Figure 2: Force-displacement cycles and temperature time history for RMP

If loading is very slow (e.g. cycling at frequency $\alpha = 0.0001$ and amplitude $\gamma = 1.2$) temperature variations are very small, the system evolves almost isothermally and the observed loop is

governed solely by the mechanical parameters. With this choice of the parameters, the isothermal pseudoelastic loop is almost flat, has a medium-high width and the plateaus are parallel (Fig. 2a).

For faster loads (e.g. $\alpha = 0.4$ and $\gamma = 1.2$) thermal effects become important as shown by the time history of the temperature in Fig. 2. It turns out that, after the transients, the temperature cycles between 1.08 and 0.95 with a mean value of 1.015. The hysteresis loop in the force-displacement plane (Fig. 2b) is thus significantly different with respect to the isothermal one. The entity of such difference is governed by the thermal parameters.

For a fixed set of model parameters, different temperature histories lead to different loop shapes that are characterized by two main effects: the almost flat plateaus become significantly steeper (henceforth this effect will be referred to as *thermal hardening*) and the area of the hysteresis loop is slightly reduced.

To develop a systematic investigation of the effect of the various model parameters on the response of the SMD and, thus, of the SMO, the following sets of parameters are considered [1].

	geometric parameters			thermal parameters			
	λ	q_1	q_2	q_3	L	h	J
RMP	8.125	0.98	1.2	constr	0.12	0.08	3.1742
MP1			1.02				
MP2		0.80					
MP3					0.01		
MP4					0.15		
MP(3+1)			1.02		0.01		
MP5						0.02	
MP6						0.20	
MP7							1.5
MP8			1.0	1.2			
MP9	6.0						

Table 2: Sets of model parameters used for comparative analysis of the response.

Since each set involves the variation of only one or two parameters with respect to the basic RMP, the comparative analysis of a synthetic indicator of response chaoticity for the various sets helps in the attempt to understand the effect of each parameter.

3 BEHAVIOR CHARTS

In order to carry out a systematic investigation of the comparative effect of the model parameters on the occurrence of chaotic responses, in the following, suitable behavior charts are computed numerically by the MWT as discussed in [7].

More specifically, both excitation frequency and amplitude are considered as control parameters. For each frequency-amplitude pair, the normalized separation between the fiduciary and perturbed trajectories is computed for the whole observation time interval.

The perturbed trajectories are obtained in each case by choosing $\varepsilon=0.0001$. The maximum value of the normalized separation in the displacement over \mathfrak{T}_1 is denoted α_{max} .

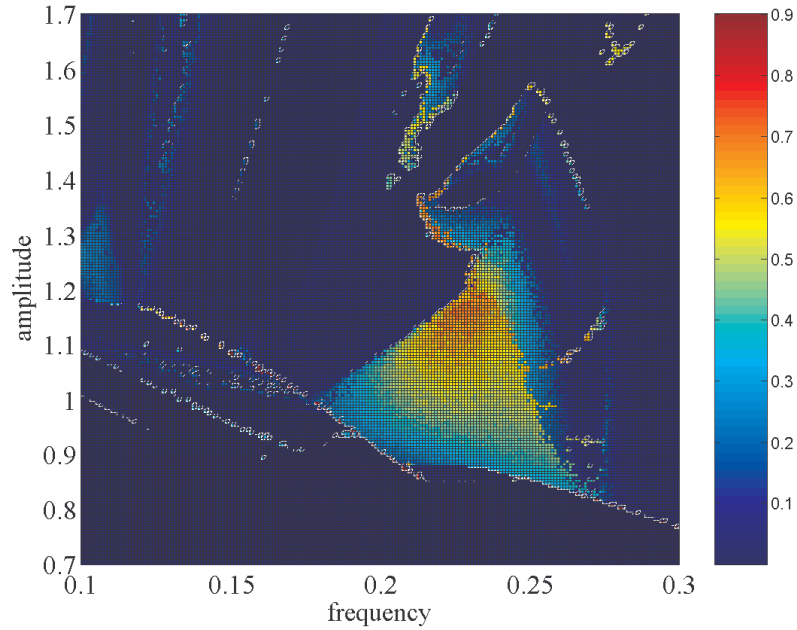


Figure 4: Behavior chart for RMP.

A *behavior chart* is then a plot of α_{max} against excitation frequency and amplitude. Each simulation is carried out at fixed initial conditions

$$\mathbf{u}_0 := [-1, -1, 0, 1, 0]$$

Behavior charts are therefore 3-dimensional plots that can be represented from various viewpoints. In the following a 2-dimensional view is preferred for the sake of clarity. Henceforth the value of α_{max} is thus represented by a color in a suitable color scale.

Figure 4 shows the behavior chart relative to the RMP case. Comparing with the results of bifurcation diagrams (herein not reported) obtained by varying either one of the two control parameters, deep blue regions in this diagram correspond to periodic solutions (α_{max} close to 0) whereas colours tending to red show increasing values of α_{max} . The greater α_{max} corresponds to non-regular solutions with higher degree of chaoticity.

Overall, it turns out that there is one main well-identified triangle shaped region of excitation frequency α and amplitude γ in which chaotic solutions occur. Within such zone, non-regular solutions show a peak of chaoticity at about $\alpha=0.22$ and $\gamma=1.2$ whereas solutions with less developed chaos arise when approaching the boundary of the region.

Besides the main zone, there are smaller scattered regions of chaos at high amplitude ($\gamma > 1.3$ and $\alpha=0.21-0.22$) as well as a chaos region at low frequency ($\alpha=0.1-0.12$ and $\gamma=1.2-1.4$), that however turns out to be of significantly lower chaoticity than the main zone.

While a more detailed analysis of the solutions is made in [8] via a systematic comparison with bifurcation diagrams and attractors, in the following, a comparative analysis of the behaviour charts obtained for the various sets of model parameters of Table 2 is presented.

The set MP1 is characterized by a decrease of the parameter q_2 that, at fixed excitation parameter values, yields a loop with less hysteresis than the RMP faster case (Fig. 2b) while

keeping a similar slope of the plateaus (Fig. 5a). In contrast, the set MP2 is characterized by a decrease of the parameter q_1 that yields a loop with more hysteresis and steeper plateaus (Fig. 5b).

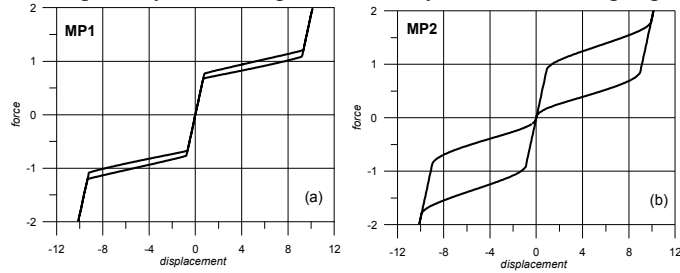


Figure 5: Force-displacement loops for MP1 and MP2 ($\alpha = 0.4$, $\gamma = 1.2$)

The reduction of hysteresis at constant plateau slope of MP1 strongly increases the extent of chaos regions as shown by the behaviour chart of Fig. 6. By comparing it with the corresponding chart of RMP (Fig. 4), a different structure of regions is also observed, in the sense that there are no longer separate zones of non-regularity because chaos can occur at almost every frequency for proper values of the excitation amplitude. Moreover, at intermediate frequencies (0.2-0.25) and amplitudes (1.0-1.2), the non-regular solutions are characterized by a comparatively very high level of chaoticity (intense red colour).

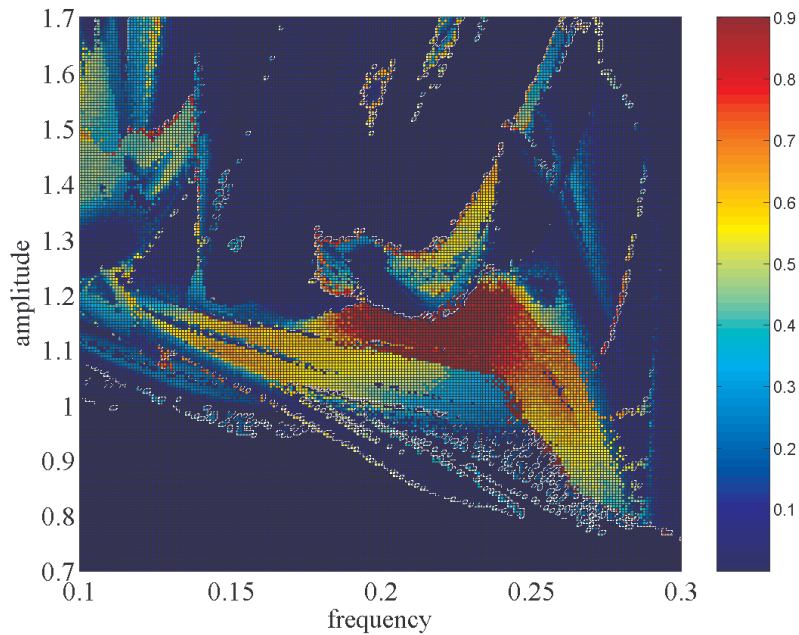


Figure 6: Behavior chart for MP1

On the contrary, the increase in both the hysteresis and pseudoelastic slopes induced by MP2 completely eliminates all the chaotic solutions (behaviour chart not included).

It is worth noting how both the two trends of modification of chaos robustness and strength, obtained by moving from RMP to MP1 or MP2 at fixed excitation parameter values (which affect the thermal features of the phase transformation process), are consistent with the qualitative

expectations ensuing from the mechanical meaning of the two varied system parameters.

In turn, the parameter sets MP3 and MP4 are characterized respectively by a decrease and a slight increase of the thermal parameter L . In particular, as shown in [1], MP3 yields almost flat plateaus, whereas MP4 emphasizes the thermal hardening, i.e. the increase of the plateaus slopes due to strong temperature variations (Fig. 7). Accordingly, somehow stronger (weaker) and more (less) robust chaos are expected with respect to RMP in the former (latter) case, which is what happens in the computer simulation results (Fig. 8). Indeed, the reduction of plateau slope induced by MP3 increases the strength of chaos within the non-regular zone, while MP4 yields a chaotic zone with similar extension as the RMP one but with lower levels of α_{max} . However, in both cases, the charts have a structure qualitatively similar to RMP, with a single major chaotic zone at intermediate frequency.

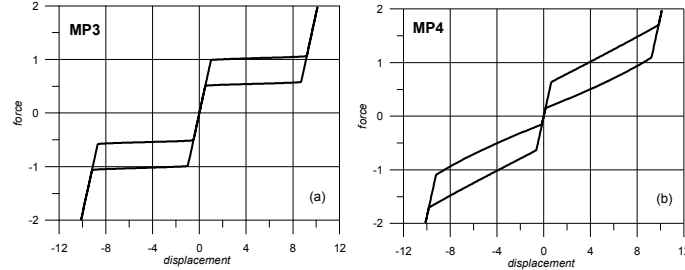


Figure 7: Force-displacement loops for MP3 and MP4 ($\alpha = 0.4$, $\gamma = 1.2$)

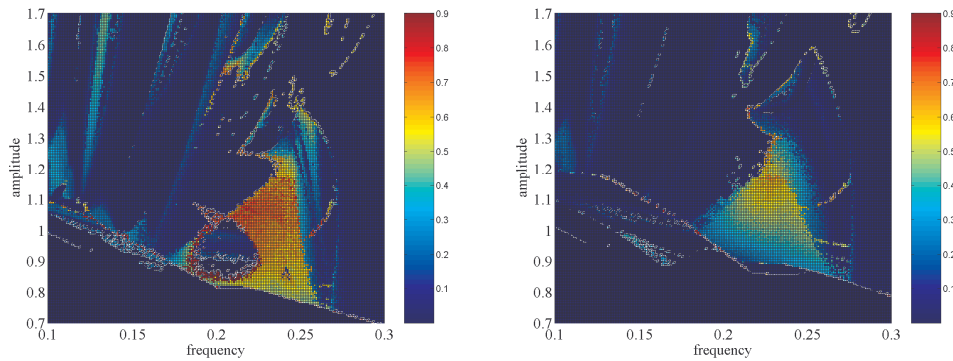


Figure 8: Behavior chart for MP3 (left) and MP4 (right)

The set MP3+1 combines the effects of MP3, that yields almost isothermal conditions (hence almost flat plateaus), and of MP1, that strongly reduces hysteresis. As expected, this turns out to be the condition with the most pronounced effects in terms of both chaos strength and chaos robustness (Fig. 9). The nearly “connected” structure of chaotic regions already observed in Fig. 6 is herein considerably enhanced.

The sets MP5, MP6 are characterized respectively by a decrease and an increase of the heat exchange coefficient h . This produces a variation of the mean value of the temperature that in the force-displacement plane is reflected into a translation of the loop toward higher or lower forces (Fig. 10). In particular MP5 relates to an environment with less convective heat exchange that produces temperature variations about a higher mean value (conversely for MP6).

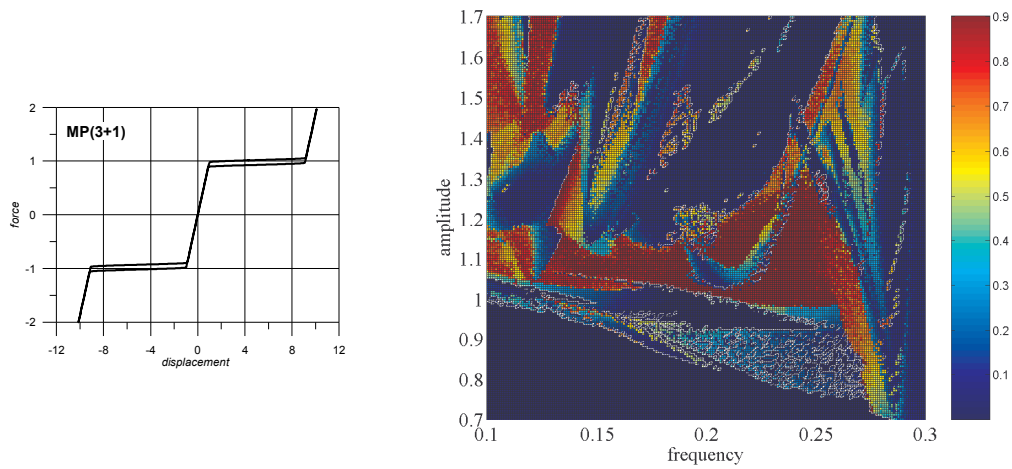


Figure 9: Force-displacement loop ($\alpha = 0.4$, $\gamma = 1.2$) and behavior chart for MP3+1

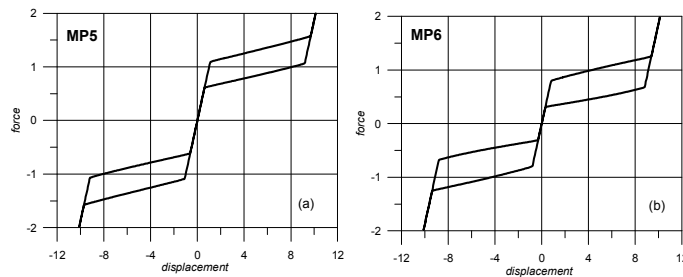


Figure 10: Force-displacement loop for MP5 and MP6 ($\alpha = 0.4$, $\gamma = 1.2$)

Overall, in both cases, a loop similar to the RMP case is obtained, since the reference h value (0.08) already lies in a range of low sensitivity to variations of the parameter [1]. Consistently, the corresponding behavior charts (Fig. 11) highlight relatively minor effects with respect to those entailed by variations of other parameters, with the overall structure of the chart being substantially similar to that obtained for RMP, namely with a main chaotic zone at intermediate frequencies and comparable values of chaoticity (mostly as regards MP6).

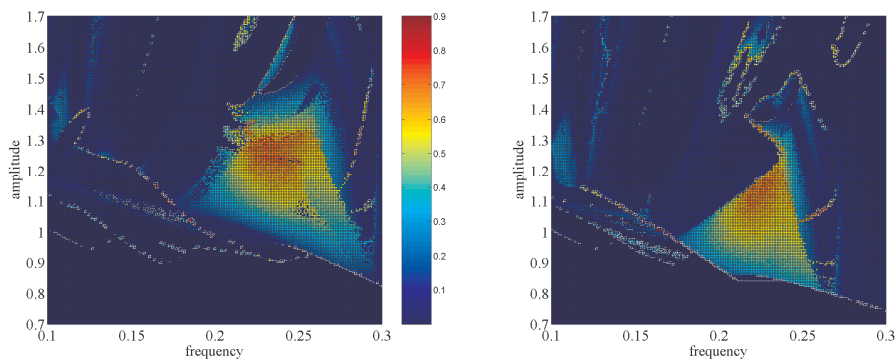


Figure 11: Behavior chart for MP5 (left) and MP6 (right)

The set MP7 increases the thermomechanical parameter J , which entails a strong reduction of the thermal effects that is reflected into a thin, flat loop [1]. This produces effects quite similar to those of MP3+1, namely a strong increase of chaos with respect to RMP. Note, however, that the source of this enhanced chaotic behaviour is completely different from that for MP3+1.

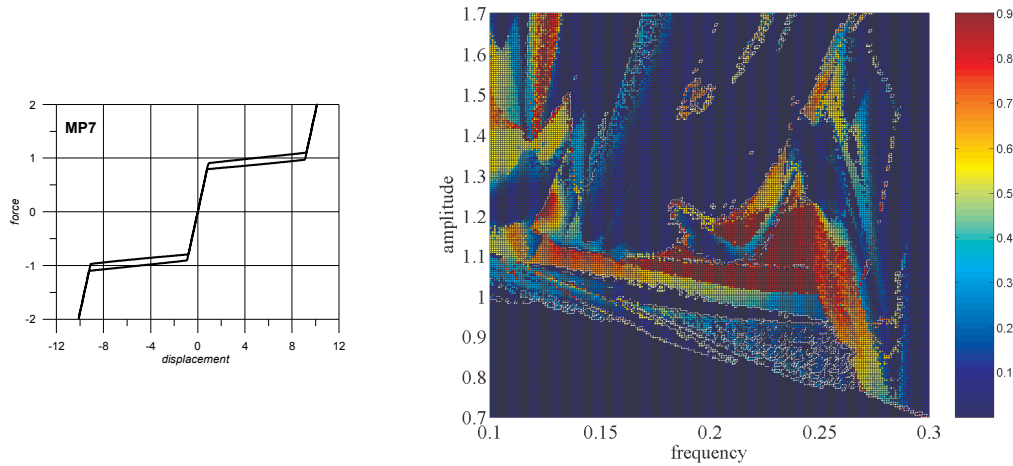


Figure 12: Force-displacement loop ($\alpha = 0.4$, $\gamma = 1.2$) and behavior chart for 7

Finally, the last two model parameter sets are MP8, that produces a loop with asymmetric plateaus (Fig. 13a), and MP9 that reduces the length of the pseudoelastic plateaus (Fig. 13b)

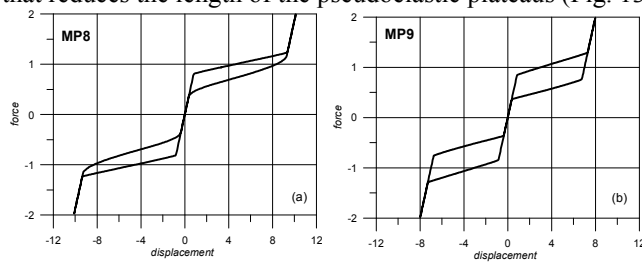


Figure 13: Force-displacement loop for MP8 and MP9 ($\alpha = 0.4$, $\gamma = 1.2$)

The loop of MP8 is characterized by a low hysteresis and, accordingly, it produces a considerable chaoticity, with non-regular solutions being again present at almost all frequencies (Fig. 14).

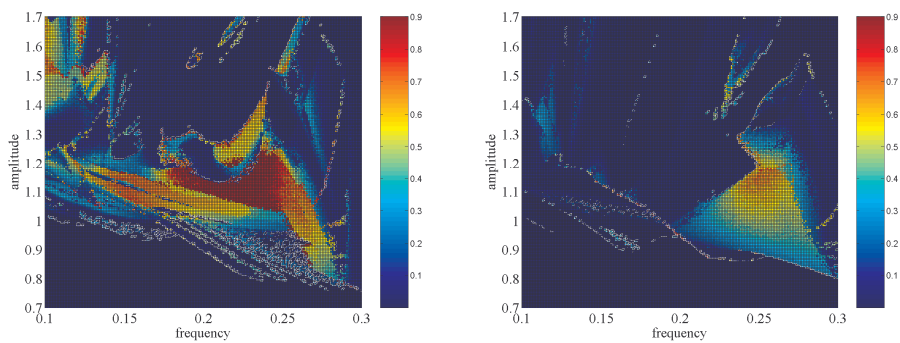


Figure 14: Behavior chart for MP8 (left) and MP9 (right)

On the contrary, the slight shortening of the plateaus, with all the other parameters remaining the same, does not produce significant variations in the behavior chart of MP9 with respect to RMP.

4 CONCLUSIONS

A systematic investigation of the effect of the thermomechanical model parameters on the nonlinear dynamic response of SMOs has been carried out in the background of theoretical predictions, by numerically computing the behavior charts for various combinations of model parameters via an enhanced version of the MWT which provides a synthetic indicator of chaoticity.

Due to the richness of the model, various modifications of the force-displacement loop can be obtained by different combinations of the parameters, with an ensuing influence on the system non-regular nonlinear dynamics which appears to be predictable mostly as regards the effects of the mechanical and of some thermal parameters. Computer simulations show that all variations involving a decrease of either hysteresis or slope of the pseudoelastic plateaus (MP1, MP3, MP3+1, MP7) yield an increase of strength and robustness of the chaotic phenomena. On the contrary, if hysteresis and slope of the plateaus have suitably high values, chaotic phenomena can be almost eliminated (MP2). Variations of other parameters such as the coefficient of heat exchange with the environment or the relative slope of the plateaus do not seem to produce significant effects on the occurrence of non-regular responses.

Besides worthily validating theoretical expectations, whether available, and providing an overall picture of the chaotic responses associated with the predictable or unpredictable effects of parameter variations, the present detailed analysis is considered to be of interest also for technical purposes in view of the design of a SMD to be used in a controlled dynamic regime.

References

- [1] Bernardini D., Rega G., The influence of model parameters and of the thermomechanical coupling on the behavior of shape memory devices, *Int. J. Non-Linear Mech.*, in press (2009).
- [2] Bernardini D., Pence T. J., Models for one-variant shape memory materials based on dissipation functions, *Int. J. Non-Lin. Mech.*, 37, 1299-1317 (2002).
- [3] Bernardini D., Rega G., Thermomechanical Modeling, Nonlinear Dynamics and Chaos in Shape Memory Oscillators, *Math. Computer Model. Dyn. Syst.*, 11, 291-314 (2005).
- [4] Machado, L. G., Savi, M. A., Pacheco, P. M. C. L.: Nonlinear dynamics and chaos in coupled shape memory oscillators. *Int. J. Solids Struct.*, 40, 5139-5156 (2003)
- [5] Lagoudas D.C., Khan M. M., Mayes J. J., Henderson B. K., Pseudoelastic SMA spring elements for passive vibration isolation: Part II – Simulations and experimental correlations *J. Intellig. Mater. Syst. Structures*, 15, 443-470 (2004)
- [6] Bernardini D., Rega G., Numerical characterization of the chaotic nonregular dynamics of pseudoelastic oscillators, in: *Modeling, Simulation and Control of Nonlinear Engineering Dynamical Systems*, Awrejcewicz J. (ed.), 25-35, Springer (2008).
- [7] Bernardini D., Rega G., A comparative indicator of response chaoticity useful for systematic application of the method of the wandering trajectories, in: *Proc. of the 10th DSTA Conference*, 12/7-10/2009, Lodz, Poland.
- [8] Bernardini D., Rega G., Chaos robustness and strength in thermomechanical shape memory oscillators: Computer simulations versus theoretical predictions, in preparation (2009).